

Original research

Functional analysis of *TLK2* variants and their proximal interactomes implicates impaired kinase activity and chromatin maintenance defects in their pathogenesis

Lisa Pavinato ^{1,2} Marina Villamor-Payà ³ Maria Sanchiz-Calvo,³ Cristina Andreoli,⁴ Marina Gay,³ Marta Vilaseca,³ Gianluca Arauz-Garfalo,³ Andrea Ciolfi,⁵ Alessandro Bruselles ⁶ Tommaso Pippucci,⁷ Valentina Prota,⁴ Diana Carli ⁸ Elisa Giorgio ^{1,9} Francesca Clementina Radio ⁵ Vincenzo Antona,¹⁰ Mario Giuffrè,¹⁰ Kara Ranguin ¹¹ Cindy Colson,¹¹ Silvia De Rubeis,^{12,13,14,15} Paola Dimartino,¹⁶ Joseph D Buxbaum,^{12,13,14,15,17,18} Giovanni Battista Ferrero,⁸ Marco Tartaglia,⁵ Simone Martinelli,¹⁹ Travis H Stracker ^{3,20} Alfredo Brusco ^{1,21}

► Additional material is published online only. To view, please visit the journal online (<http://dx.doi.org/10.1136/jmedgenet-2020-107281>).

For numbered affiliations see end of article.

Correspondence to Professor Alfredo Brusco, Department of Medical Sciences, University of Turin, Torino 10124, Italy; alfredo.brusco@unito.it

THS and AB contributed equally.

Received 16 June 2020
Revised 19 October 2020
Accepted 14 November 2020



© Author(s) (or their employer(s)) 2020. No commercial re-use. See rights and permissions. Published by BMJ.

To cite: Pavinato L, Villamor-Payà M, Sanchiz-Calvo M, *et al.* *J Med Genet* Epub ahead of print: [please include Day Month Year]. doi:10.1136/jmedgenet-2020-107281

ABSTRACT

Introduction The Tousel-like kinases 1 and 2 (TLK1 and TLK2) are involved in many fundamental processes, including DNA replication, cell cycle checkpoint recovery and chromatin remodelling. Mutations in *TLK2* were recently associated with 'Mental Retardation Autosomal Dominant 57' (MRD57, MIM# 618050), a neurodevelopmental disorder characterised by a highly variable phenotype, including mild-to-moderate intellectual disability, behavioural abnormalities, facial dysmorphism, microcephaly, epilepsy and skeletal anomalies.

Methods We re-evaluate whole exome sequencing and array-CGH data from a large cohort of patients affected by neurodevelopmental disorders. Using spatial proteomics (BioID) and single-cell gel electrophoresis, we investigated the proximity interaction landscape of *TLK2* and analysed the effects of p.(Asp551Gly) and a previously reported missense variant (c.1850C>T; p.(Ser617Leu)) on TLK2 interactions, localisation and activity.

Results We identified three new unrelated MRD57 families. Two were sporadic and caused by a missense change (c.1652A>G; p.(Asp551Gly)) or a 39 kb deletion encompassing *TLK2*, and one was familial with three affected siblings who inherited a nonsense change from an affected mother (c.1423G>T; p.(Glu475Ter)). The clinical phenotypes were consistent with those of previously reported cases. The tested mutations strongly impaired *TLK2* kinase activity. Proximal interactions between TLK2 and other factors implicated in neurological disorders, including CHD7, CHD8, BRD4 and NACC1, were identified. Finally, we demonstrated a more relaxed chromatin state in lymphoblastoid cells harbouring the p.(Asp551Gly) variant compared with control cells, conferring susceptibility to DNA damage.

Conclusion Our study identified novel *TLK2* pathogenic variants, confirming and further expanding the MRD57-related phenotype. The molecular characterisation of missense variants increases our knowledge about

TLK2 function and provides new insights into its role in neurodevelopmental disorders.

INTRODUCTION

The Tousel-like kinases 1 and 2 (TLK1 and TLK2) are serine-threonine kinases involved in DNA replication and repair, transcription, cell cycle checkpoint recovery, chromatin maintenance and genomic stability.^{1–3} Both kinases target the ASF1A and ASF1B histone H3/H4 chaperones and are regulated by DNA damage responsive checkpoint signalling.⁴ Depletion of *Tlk1* and *Tlk2* in mice indicated that they are largely redundant, with the exception of an essential role for *Tlk2* in placental development.⁵ Null *Tlk2* mice, generated with a conditional allele to bypass the placental defect, showed no gross developmental defects except for a slight growth delay compared with controls, suggesting that TLK1 can compensate for loss of TLK2 function after embryonic development. Further work in human cancer cells supports extensive redundancy at the cellular level. Co-depletion of TLK1 and TLK2, however, causes replication stress, DNA damage and altered chromatin maintenance, particularly affecting telomeres and other repetitive genome elements, while mild effects were observed with depletion of either protein.⁶

Mutations in *TLK2* were associated with Mental Retardation Autosomal Dominant 57 (MRD57, MIM# 618050) by Reijnders *et al.*,⁷ who described 40 cases from 38 unrelated families. MRD57 is clinically characterised by autism spectrum disorder (ASD), intellectual disability (ID), behavioural problems, growth delay and facial dysmorphism, including blepharophimosis, telecanthus, prominent nasal bridge, broad nasal tip, thin vermilion of the upper lip and upslanting palpebral fissures. Other features shared by a subset of cases are

gastrointestinal problems, seizures, skeletal malformations and ocular problems.

In the majority of reported cases, the disease is likely due to *TLK2* haploinsufficiency, as most of cases are heterozygous for loss-of-function (LoF) alleles, which is in line with the strong constraint against LoF variants in the gene (pLI=1, GnomAD database). Reported missense variants cluster mainly in the C-terminal protein kinase domain (PKD),⁷⁻⁹ the core of *TLK2* function. Four *TLK2* variants localised in this region have previously been analysed, showing a strong reduction of kinase activity on ASF1A *in vitro*.¹⁰ *TLK2* activation requires dimerisation through an N-terminal coiled coil motif, suggesting that inactive mutants could have a dominant negative effect.¹⁰ Thus, based on the available data, the predominant pathogenic mechanism of *TLK2* mutations appears to be a reduction in its overall activity. Of note, recent work suggested a possible autosomal recessive phenotype in a proband affected by severe neurodevelopmental disease with a homozygous missense variant (c.163A>G; p.(Lys55Glu)).⁸ This variant is localised outside the *TLK2* PKD and coiled-coil motifs, and may be hypomorphic, since the carrier parents are not affected.

During the screening of a large survey of patients with ID by array-CGH and whole exome sequencing (WES), we identified three new cases with *TLK2*-mutations. Two subjects were heterozygous for a de novo 39 kb deletion encompassing *TLK2*, and a de novo c.1652A>G; p.(Asp551Gly) missense change. The third case was familial, with a nonsense variant (c.1423G>T; p.(Glu475Ter)) occurring in three affected siblings and their affected mother. Here, we report their clinical description, confirming and expanding the disease phenotype. We also provide data documenting an altered chromatin state in patient-derived fibroblasts and lymphoblastoid cells (LCLs), consistent with a defect in the regulation of histone chaperones. Finally, we characterised the activity and proximal interactomes of the p.(Asp551Gly) variant, as well as another missense variant (p.(Ser617Leu)), reported in a several published studies.¹¹⁻¹³ Both variants exhibited impaired kinase activity and *TLK2* proximal interactomes were enriched with proteins previously implicated in ID and ASD, suggesting connections to a larger chromatin maintenance network.

MATERIALS AND METHODS

Whole exome sequencing, prioritisation and variant calling

DNA was extracted from total blood using the ReliaPrep Blood gDNA Miniprep kit (Promega, Madison, Wisconsin, USA) following manufacturer's protocol and quantified with a NanoDrop spectrophotometer (Thermo Fisher Scientific, Waltham, Massachusetts, USA).

Array-CGH was performed using a 60K whole-genome oligonucleotide microarray (Agilent Technologies, Santa Clara, California, USA). Family 1 and 2 were enrolled in the Autism Sequencing Consortium (ASC) project and their gDNA samples were sequenced at the Broad Institute on Illumina HiSeq sequencers as previously described^{11 14}; variant calling was performed using targeted bioinformatic pipelines adapted for different pattern of inheritance. Identified variants were confirmed by Sanger sequencing using standard conditions and the primers in online supplemental table S1. Additional information is provided in online supplemental materials and methods.

All variants are referred to GRCh37 annotation and to NM_001284333.2, in line with the previously published *TLK2* structure.¹⁰ For homogeneity with the clinical work from

Reijnders *et al*,⁷ we specified variants also in NM_006852.6 in online supplemental table S2.

In silico prediction of missense variants impact and splicing analysis

Variants were analysed with the VarSome tool¹⁵ as a starting point for further analysis. This allowed evaluation of at least 15 *in silico* predictors simultaneously. Variants frequencies were evaluated using Genome Aggregation Database (GnomAD) Browser V.2.1.1. Impaired splicing was predicted using Human Splicing Finder V.3.1¹⁶ and experimentally verified as described in online supplemental materials and methods.

Cell cultures

Peripheral blood mononuclear cells were isolated from whole blood using Histopaque-1077 (Sigma-Aldrich) and subsequently immortalised with Epstein-Barr virus and cultured in RPMI medium (Gibco, Thermo Fisher Scientific) supplemented with 10% fetal bovine serum (FBS) (Gibco), 1% penicillin-streptomycin and 1% L-glutamine. Primary fibroblasts were isolated from human skin biopsies after overnight incubation in Dulbecco's Modified Eagle's Medium (DMEM) (Sigma-Aldrich) supplemented with 10% FBS and 160 µg/mL collagenase. Fibroblasts were maintained in DMEM supplemented with 10% FBS, 1% penicillin-streptomycin and 1 mM sodium pyruvate (Thermo Fisher Scientific) at 37°C, 5% CO₂. AD-293 cells (Stratagene) were grown in DMEM supplemented with 10% FBS (Sigma-Aldrich), 50 U/mL penicillin and 50 µg/mL streptomycin (Thermo Fisher Scientific) at 37°C in a 5% CO₂ incubator.

RNA isolation and quantitative real-time PCR

Total RNA was extracted from fibroblasts and LCLs using the Direct-Zol RNA MiniPrep system (Zymo Research, Irvine, California, USA) and cDNA was generated using the M-MLV Reverse Transcriptase kit (Invitrogen, Thermo Fisher Scientific). The expression level of *TLK2* was measured using the Universal Probe Library system (Roche Diagnostics, Risch-Rotkreuz, Switzerland) with primers and probe in online supplemental table S1 and *HMBS* and *GAPDH* as reference gene (assays numbers Hs00609297_m1 and Hs00266705_g1; Applied Biosystems, Thermo Fisher Scientific). Assays were carried out in triplicate on an ABI 7500 real-time PCR instrument using the ABI 2X TaqMan Universal PCR Master Mix II, according to the manufacturer's protocol (Thermo Fisher Scientific). For each experiment, biological triplicates with at least two technical replicates were performed. Data were analysed with Prism-GraphPad Software performing unpaired t-test with Welch's correction. P values are indicated as follows: ns=p>0.05; *p<0.05; **p<0.01; ***p<0.001; ****p<0.0001.

Single-cell gel electrophoresis

Samples were prepared according to the alkaline single-cell gel electrophoresis (SCGE) assay method, as previously described¹⁷ and are briefly summarised in online supplemental material and methods, together with experimental details.

Site directed mutagenesis and *in vitro* kinase assays from cell lysates

In vitro kinase assays were performed as previously described¹⁰ with minor modifications. Full methods are provided in the online supplemental materials and methods and primers in online supplemental table S3.

Western blot analysis

For affinity purification (AP), 40 µg of input protein and 20 µL of Strep-AP elution, with 6X SDS (0.2% bromophenol blue and β-mercaptoethanol), were separated by SDS-PAGE and transferred to nitrocellulose membranes (0.2 or 0.45 µm pore, Amersham Protran; Sigma-Aldrich). For detection of streptavidin, polyvinylidene fluoride membranes (0.45 µm pore, Immobilon-P, Merck) were used. Membranes were blocked and antibodies prepared in 5% non-fat milk in PBS-Tween20 (PBS-T), with the exception of CHD7 and CHD8, where 5% bovine serum albumin in PBS-T was used. Primary antibodies were detected with the appropriate secondary antibodies conjugated to horseradish peroxidase (HRP) (online supplemental table S4) and visualised by ECL-Plus (GE Healthcare).

Proximity-dependent biotin identification mass spectrometry (BioID-MS)

BioID-MS and BioID-westerns were performed essentially as described in the study by Silva *et al*¹⁸ with some modifications. Full methods are provided in the online supplemental materials and methods and data are available in the PRIDE database with accession number PXD019450.

RESULTS

Identification of novel *MRD57* patients

The identification of *TLK2* as a risk gene for Intellectual Disability (ID),⁷ prompted us to re-evaluate the genomic information available for a large cohort of patients affected by ASD and/or ID who had previously been analysed by WES. This included our in-house cohort (2250 total samples, 736 affected), as well as a publicly available one from the ASC (35 584 total samples, 11 986 affected).¹¹ No further likely pathogenic variants or variant of unknown significance in neurodevelopment-related genes² were identified. A search in the DECIPHER database¹⁹ for novel *TLK2* deletions was also performed. We found six cases in three independent families with detrimental variants in the *TLK2* gene (figure 1A–F).

In family 1, the proband carried a de novo missense change c.1652A>G; p.(Asp551Gly) not reported in gnomAD and predicted to be damaging by multiple *in silico* predictors (online supplemental table S5). This variant localises in a highly Constrained Coding Region (CCR) (>93th percentile) within the PKD.²⁰ In family 2, three affected siblings carried a premature stop variant (c.1423G>T; p.(Glu475Ter)) inherited from their affected mother (case 2). This variant was not reported in gnomAD and was classified as pathogenic using the American College of Medical Genetics (ACMG) criteria.^{7,8} A sixth case (family 3) was identified in the DECIPHER database: a female carried a likely pathogenic (class 4)^{7,8} de novo del(17)(q23.2), whose minimum size was 39 kb (NC_000017.10:g.(60683462–60722398)del). The deletion encompassed *TLK2*, *MRC2* and *MARCH10* genes. Neither the *MRC2* nor *MARCH10* genes are predicted to be haploinsufficient (GnomAD *MRC2* pLI=0.67; *MARCH10* pLI=0). *MRC2* encodes the Mannose Receptor C Type 2 and has a role in the turnover of collagens in the cytomembrane and extracellular matrix.⁸ Its upregulation has been linked to tumourigenic activity, and a role in breast cancer and hepatocellular carcinoma has been suggested^{9,10} but, to our knowledge, there is no supporting literature implicating *MRC2* in neurodevelopmental disorders. The literature available for *MARCH10* is limited but the gene is expressed almost exclusively in testis (<https://gtexportal.org/home/gene/MARCH10>) and was suggested to play a role in spermiogenesis.¹¹ Therefore, we think

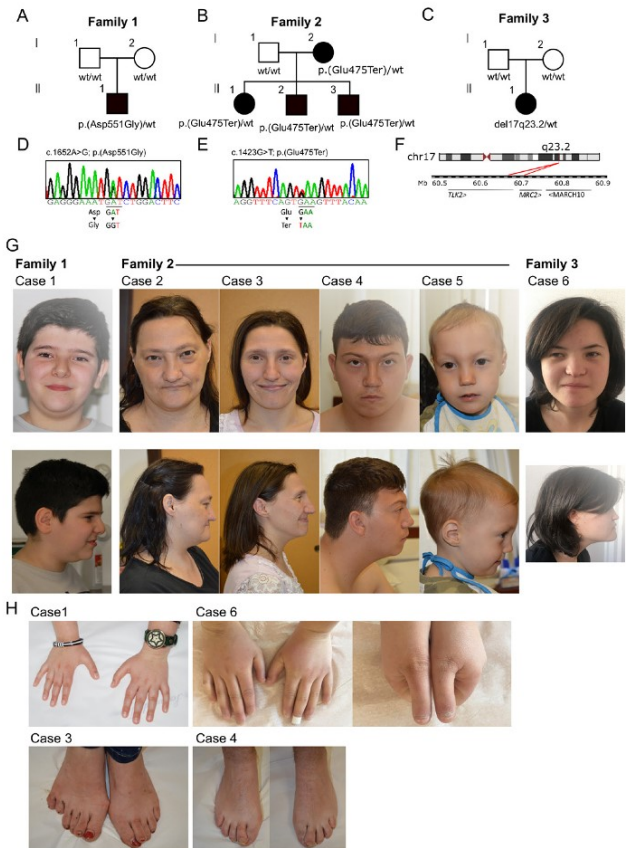


Figure 1 Facial features and skeletal anomalies of individuals with *TLK2* variants. (A–C) Pedigrees of family 1, 2 and 3. Cases from family 1 and 3 carried respectively a heterozygous de novo missense variant (c.1652A>G; p.(Asp551Gly)) and a heterozygous de novo deletion encompassing *TLK2* gene. Cases from family 2 shared a heterozygous premature stop variant (c.1423G>T; p.(Glu475Ter)) inherited from an affected mother. Analysis of maternal grandparent genotype were not possible, but familial clinical history did not suggest a possible MRD57-like phenotype for them. wt, wild type at variant position. (D–E) Sanger validation of variants identified in family 1 and 2. Validation was performed both on gDNA from affected cases and from their unaffected relatives. (F) 17q23.2 deletion (minimum size 39 kb, chr17-60683462–60722398) identified in case 6 from family 3. The 39 kb deletion encompassed *TLK2* and *MRC2* genes. (G) Frontal and lateral face photographs of our cases, showing overlapping facial dysmorphisms. Most frequently reported features were upward slanted palpebral fissures, broad nasal tip, thin lips, low hanging columella, prognathism, wide spaced eyes and downturned corners of the mouth. (H) Details of reported skeletal anomalies at the level of hands and feet. Upper left panel: tapered hands fingers from case 1; upper right panels: short hands with short distal phalanx from case 6; bottom left panel: postaxial polydactyly of left foot observed in case 3; bottom right panel: overriding second toe in case 4.

it is unlikely that haploinsufficiency in *MRC2* or *MARCH10* contribute to the patient's phenotype.

Our patients (three males and three females) ranged from 3 to 47 years of age, all of them were of Caucasian ethnicity. A broad range of behavioural disorders was present, including ASD (1/6), attention deficit hyperactivity disorder (4/6), anxiety (3/6), short attention span (2/6) and obsessive-compulsive behaviour (2/6). ID was reported for four patients in the borderline (IQ 70–85) or low (IQ ≤70) range. Patient 5 was too young for

formal assessment of a neurodevelopmental phenotype, but a global developmental delay was reported. No formal evaluation for ID was provided for case 6 but difficulties in memory and transcription were reported. All affected members from family 2 had microcephaly. Dysmorphic facial features were observed in all patients and included upslanting palpebral fissures, wide nose, low hanging columella, smooth philtrum, prognathism, pointed chin and hypertelorism (figure 1G). Minor skeletal anomalies of the hands and feet were reported for four patients (figure 1H). Interestingly, some of the features we observed in a portion of our patients had not been described in previously reported cases, expanding the clinical phenotype. Among them, there were neurodevelopmental (difficulties in reading, writing, memory and transcription and pavor nocturnus), dysmorphic (prognathism, bifid nasal tip, low hanging columella, absent ear lobe, low-implant auricle, synophrys and downturned corners of mouth) and skeletal anomalies (postaxial polydactyly of left foot, overriding second toe, tapering fingers, short hands with short distal phalanx). A summary of the clinical phenotypes is reported in online supplemental table S6 and a description is provided in the online supplemental data, while a comparison with the available literature is provided in online supplemental table S7.

TLK2 haploinsufficiency disrupts proper chromatin compaction

Using qRT-PCR, we analysed *TLK2* mRNA expression in LCLs from case 1 and fibroblasts from case 6. We found an approximately 50% reduction in *TLK2* mRNA expression in both cases (figure 2A and online supplemental figure S1A). This was unexpected in case 1, who carried the c.1652A>G; p.(Asp551Gly) missense change. Variants encoding missense changes may induce unstable mRNA secondary structures leading to degradation of the altered allele.^{8,9} To verify if both alleles were expressed, we amplified and sequenced cDNA between exons 18 and 23. We found that both wild-type (WT) and mutant allele were present (online supplemental figure S1B), suggesting that the allele encoding the p.(Asp551Gly) variant was not degraded. Moreover, no differences were observed in band sizes from WT and p.(Asp551Gly) cDNAs (online supplemental figure S1C), excluding that p.(Asp551Gly) led to the production of aberrantly spliced transcripts.^{21,22} Western blot analysis on LCLs from case 1 compared with controls, uncovered a significant increase in TLK2 protein expression (online supplemental figure S1D), motivating us to perform a deeper characterisation of the impact of p.(Asp551Gly) on TLK2 activity.

Based on the role of TLK2 in controlling chromatin remodelling,² we investigated possible changes in chromatin compaction, performing the SCGE assay with LCLs derived from case 1. Relatively short electrophoresis time was already sufficient to unmask slight differences between control and mutant cells. Longer run times allowed DNA loops to stretch under the electric field and revealed a significantly more relaxed state of nucleoids in LCLs from the affected subject compared with control cells (figure 2B,C). Differences were quantified as ‘tail moment’ values, which are defined as the product of the tail length and the percentage of DNA in the tail. LCLs harbouring the p.(Asp551Gly) variant also exhibited a higher sensitivity to γ -ray irradiation, documenting increased susceptibility to DNA damage (ie, single and double strand breaks), which is in line with a more relaxed state of chromatin (figure 2D and E). Of note, a defective heterochromatin state was also observed in fibroblasts derived from subject 6 carrying the 17q23.2

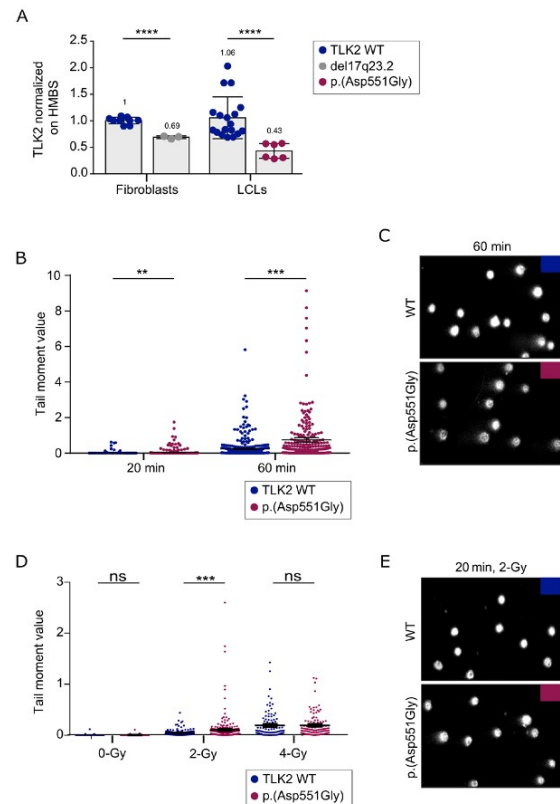


Figure 2 TLK2-Asp551Gly affects chromatin density and confers susceptibility to DNA damage. (A) *TLK2* mRNA levels in fibroblasts from case 6 and in lymphoblastoid cell line derived from case 1. *TLK2* expression was significantly reduced both in lymphoblastoid cell (LCL) carrying p.(Asp551Gly) variant and in fibroblasts carrying the 17q23.2 deletion. All experiments were performed at least in triplicate. UPL probe #72 and primers indicated in online supplemental materials and methods were used; *HMBS* mRNA expression was used as reference. Statistical analysis was performed using t-test with Welch's correction; **** $p \leq 0.0001$. Numbers at the top of the bars indicated mean values. (B) Single-cell gel electrophoresis (SCGE) assays highlighted significant differences in chromatin condensation between LCLs carrying the p.(Asp551Gly) amino acid change and control cells after 20 min of electrophoresis run time (** $p < 0.05$; two-tailed unpaired Student's t-test with Welch's correction), that became more evident after 60 min of electrophoresis run time (*** $p \leq 0.0001$; two-tailed unpaired Student's t-test with Welch's correction). DNA migration was quantified as Tail moment values, which is defined as the product between the tail length and the percentage of DNA in the tail. For each point, at least 100 cells were analysed. Values are represented as mean \pm SEM of three independent experiments. (C) Representative images of nucleoids derived from control LCLs and LCLs from affected subject 1 referred to experiment shown in (B). (D) Single and double strand breaks were induced by γ -ray irradiation (2 Gy or 4 Gy). Tail moment values specify the amount of γ -ray-induced DNA damage measured immediately after the treatment. The mutant LCLs showed a higher vulnerability to 2 Gy γ -ray irradiation (*** $p \leq 0.0006$; two-tailed unpaired Student's t-test with Welch's correction). Following 4 Gy treatment, no differences were observed between control and mutant cells, which is likely explained by the observation that the overall damage, especially double strand breaks, prevails on the condensation state of chromatin at high doses of γ -ray irradiation. For each point, at least 100 cells were analysed and four independent experiments were performed. (E) Representative images of nucleoids derived from control LCLs and LCLs from affected subject 1 referred to experiment shown in (D). ns, not significant.

deletion encompassing *TLK2* (online supplemental figure S2), suggesting a similar effect between the 17q23.2 deletion and the p.(Asp551Gly) variant. Overall, these findings demonstrated that *TLK2* haploinsufficiency disrupts proper chromatin organisation and confers susceptibility to DNA damage.

TLK2 missense mutations alter the activity and subcellular localisation of the protein

All of the *TLK2* missense mutations in the PKD from MRD57 analysed to date exhibited decreased kinase activity, including H493R, H518R, R720A and D629N¹⁰ (online supplemental figure S4B). Given that the high conservation of the mutated residues in the PKD suggested reduced kinase activity, we examined the potential structural impact of the missense p.(Asp551Gly) (hereafter indicated as D551G) variant identified in our survey, as well as the p.(Ser617Leu) (hereafter indicated as S617L) variant, found in a patient with ASD already described in WES works.^{11–13} The patient was also reported in the ASC exome analysis browser, a freely accessible portal containing de novo variants identified in >6000 affected probands enrolled in ASC WES projects (<https://asc.broadinstitute.org/>). Residue S617 is located one residue after the Asp-Phe-Gly (DGF) motif,^{23 24} which together with the activation and catalytic loop, constitute the kinase core.¹⁰ We previously identified S617 as a *TLK2* autophosphorylation site and demonstrated that alterations of this site are able to significantly enhance (S617A) or reduce (S617D) *TLK2* kinase activity.¹⁰ Therefore, it remained an open question how S617L, associated with ASD, would influence the kinase activity of *TLK2*.

We modelled both of the mutations using the crystal structure of the *TLK2* PKD.¹⁰ *TLK2*-D551G was predicted to weaken hydrogen bonds with the subsequent helix and S617L introduces a hydrophobic residue in place of the autophosphorylation site in the activation loop (figure 3A,B).

To determine if these mutations affected kinase activity, we analysed *TLK2* activity using in vitro kinase assays. Ectopically expressed, Strep-FLAG tagged *TLK2*, *TLK2*-KD (kinase dead, D592V), *TLK2*-D551G and *TLK2*-S617L were affinity purified from AD-293 cells using an N-terminal Strep tag and incubated with purified substrate (ASF1A) for kinase assays. Both mutations led to a notable reduction in substrate modification (figure 3C,D). Quantification of multiple experiments demonstrated that *TLK2*-S617L severely impaired kinase activity, comparable to the *TLK2*-KD protein, while *TLK2*-D551G was more mildly impaired and showed slightly higher autophosphorylation levels than *TLK2*-WT in some experiments (figure 3D).

In previous work, we noted that loss of the coiled-coil domains of *TLK2* led to perinuclear accumulation.¹⁰ To determine if the *TLK2*-D551G and *TLK2*-S617L missense mutations altered *TLK2* localisation, we transfected FLAG-tagged mutants in AD-293 cells and performed immunofluorescence (IF) microscopy. Lamin A was used as an inner nuclear membrane marker and nuclear DNA was stained with DAPI. *TLK2*-WT showed diffuse nuclear localisation in transfected cells, as observed previously (figure 3E, online supplemental figure S3A). In contrast, *TLK2*-D551G and *TLK2*-S617L showed perinuclear localisation to different extents (figure 3E,F, online supplemental figure S2A). This was particularly prominent for the *TLK2*-S617L mutant, where 75% of transfected cells showed a perinuclear localisation of *TLK2* (figure 3E,F).

Figure 3

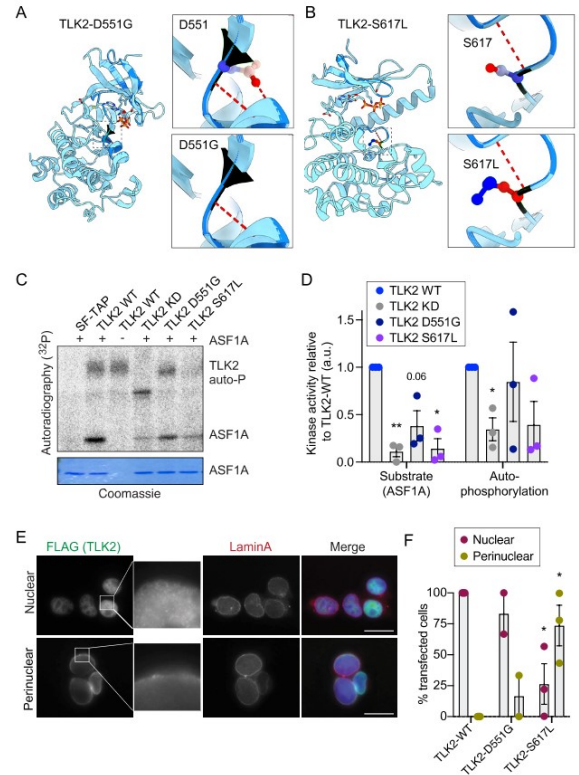


Figure 3 *TLK2* autism mutations alter the activity and subcellular localisation of *TLK2*. (A–B) Modelling of the D551G and S617L missense mutations on the crystal structure of the *TLK2* protein kinase domain (PKD). Hydrogen bonds are shown in red dashed lines. (C) Representative in vitro kinase assays with Strep-purified *TLK2*-wild-type (WT), *TLK2*-KD (kinase dead; D592V) and indicated missense variants. Autophosphorylation and substrate (ASF1A) phosphorylation is shown. Coomassie is shown as loading control for ASF1A. (D) Quantification of $n=3$ independent kinase assays. Individual results (circles) are shown for each assay on purified ASF1A substrate or affinity purified *TLK2* autophosphorylation relative to corresponding *TLK2*-WT and bars depict mean with SEM. (E) Representative immunofluorescence microscopy of overexpressed *TLK2* in AD-293 cells is shown, indicating the two main localisation patterns observed. The nuclear localisation image corresponds to *TLK2*-WT, while the perinuclear localisation to *TLK2*-S617L. Scale bar=20 μ m. (F) Quantification of *TLK2* localisation patterns for WT and indicated missense variants. Ten random fields were scored in 2 (D551G) or 3 (WT and S617L) biological replicates. Bars depict mean with SEM. Statistical significance was determined using an unpaired t-test with Welch's correction (**** $p<0.0001$, *** $p<0.001$, ** $p<0.01$, * $p<0.05$).

The proximal interactome of *TLK2* is altered by missense mutations

TLK2 is involved in many biological processes and few clear substrates aside from ASF1A and ASF1B have been well characterised.² As kinases often bind to substrates with low affinity, we previously used an unbiased proximity biotinylation assay coupled to mass spectrometry (BioID-MS), as it does not require high-affinity interactions that can withstand purification procedures.^{5 25} We used this approach to further characterise the

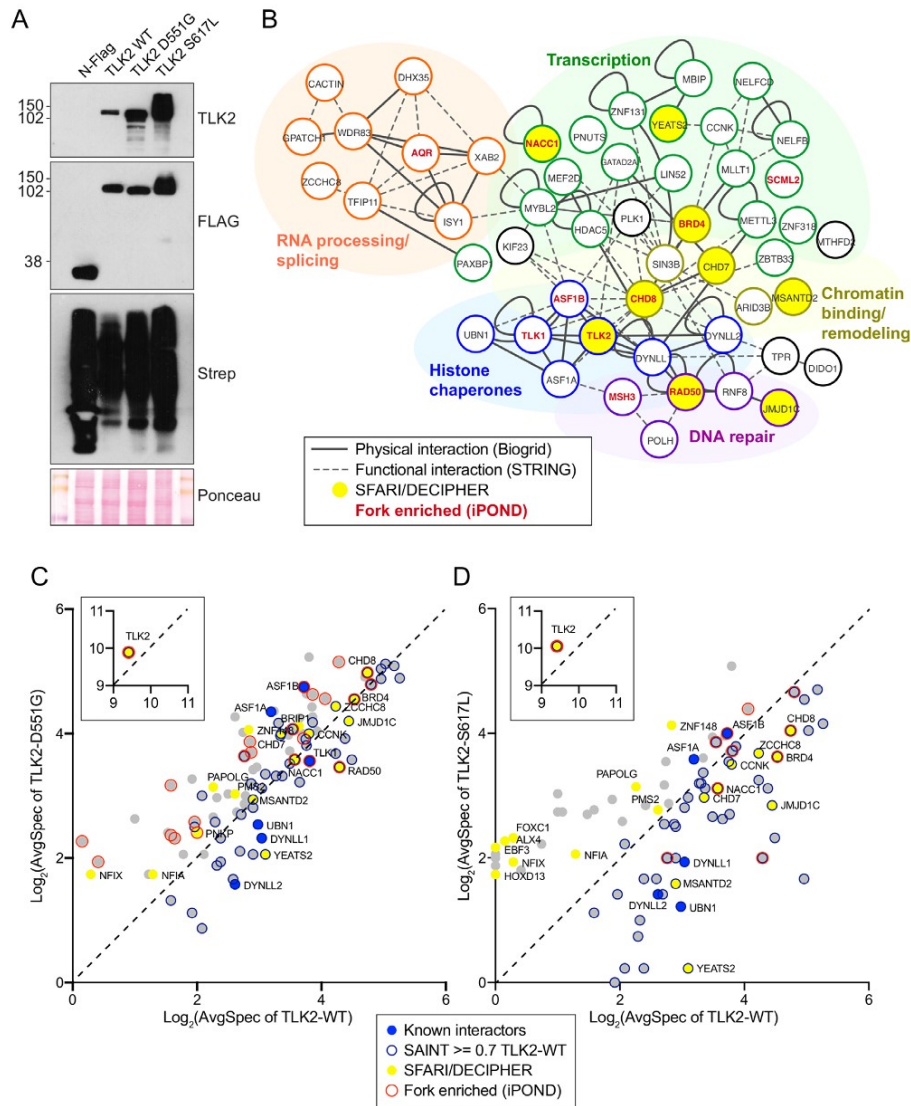


Figure 4 Biold-based analysis of the proximal interactome of TLK2. (A) Western blot analysis of AD-293 lysates expressing Biold constructs: N-FLAG-BirA alone or fused to the indicated TLK2 allele. Detection with anti-TLK2, anti-FLAG or streptavidin-horseradish peroxidase are shown. Ponceau stained nitrocellulose membrane is shown as a loading control. (B) Network clustering of all prey hits with a SAINT score of ≥ 0.7 in TLK2-WT samples. Physical interactions reported in Biogrid (solid lines) and functional interactions (dashed lines) reported in STRING are indicated.^{43 44} Functionally enriched clusters are indicated by colour coding, Bait, TLK2 substrates, proteins found in the Simon's Foundation Autism Research Initiative (SFARI)/DECIPHER gene database (yellow fill) or proteins enriched on nascent DNA/replication forks are indicated (red font). (C–D) Scatter plots of average spectral counts (Log_2 transformed) of bait and prey proteins identified with the TLK2-D551G and TLK2-S617L alleles compared with TLK2-WT. Previously identified TLK2 interactors, as well as proteins enriched on replication forks or found in the SFARI/DECIPHER databases are indicated (see legend).

cellular environment of TLK2 and determine if the missense mutations influenced its interactome.

BirA-tagged *TLK2-WT*, *TLK2-D551G* and *TLK2-S617L* were expressed in AD-293 cells by transient transfection (figure 4A). Network clustering of results from WT TLK2 (TLK2-WT) identified the known TLK2 substrates ASF1A, ASF1B and TLK1, as well as the DYNLL1/2 (LC8) proteins that we previously validated.^{5 10} The proximal interactome grouped into five functional clusters consistent with the known functions of TLK2, including RNA processing and splicing, transcriptional regulation, chromatin binding or remodelling, DNA repair and histone chaperones (figure 4B and online supplemental table S8). We cross-referenced the proximal interactome with a recent large-scale analysis of

iPOND-MS data that identified TLK1 and TLK2 as high confidence interactors with nascent DNA at active replication forks.²⁶ Several of the TLK2-WT hits, including RAD50, BRD4, CHD8, ASF1B, SCML2 and NACC1 were also found at active forks with high confidence in iPOND studies. We next compared our TLK2-WT proximal interactome with the Simon's Foundation Autism Research Initiative (SFARI) and DECIPHER databases and identified eight proteins: CHD7, CHD8, NACC1, CCNK, JMJD1C, RAD50, MSANTD2 and YEATS2. These data suggest potential functional links between TLK2 and a number of proteins involved in neurodevelopmental disorders with overlapping pathologies. Details about SFARI and OMIM classifications are provided in online supplemental table S9.

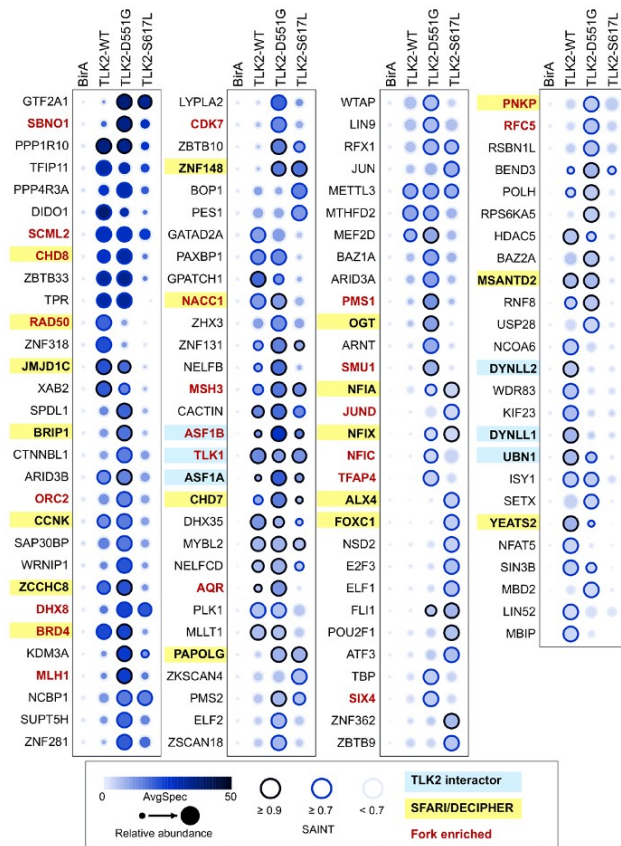


Figure 5 Missense variants alter the proximal interactome of TLK2. (A) Dot plot of prey proteins with a SAINT score of ≥ 0.7 with any of the three baits generated using ProHits-viz.⁴⁵ Average spectral counts (SC), relative abundance and SAINT score ranges are indicated, as well as proteins enriched on replication forks²⁶ or found in the Simon's Foundation Autism Research Initiative (SFARI)/DECIPHER databases (see legend). Additional details are provided in online supplemental table S8.

In parallel to TLK2-WT, we performed BioID analysis with TLK2-D551G and TLK2-S617L. Both mutants accumulated to higher levels than TLK2-WT, consistent with what we previously observed with other inactive TLK2 mutants.¹⁰ Both mutants caused numerous alterations in the proximal interactions compared with TLK2-WT (figures 4C,D and 5). This included a reduction in several replication fork and ASD-related proteins, including RAD50 and YEATS2 with both mutants, and JMJD1C, BRD4, CCNK, NACC1, MSANTD2 and CHD8 with TLK2-S617L (figures 4 and 5). In addition, some proteins, including ZNF148, NFIA, NFIX and PAPOLG, that are all in the SFARI database, were significantly enriched with both mutants, but not TLK2-WT. (figures 4C,D and 5)

The CHD7 and CHD8 chromodomain helicases were of particular interest to us because they are mutated respectively in CHARGE syndrome²⁷ (MIM# 214800) and susceptibility to autism²⁸ (615032) and implicated in modulating chromatin structure.^{29,30} In addition, CHD8 has been localised to active sites of DNA replication, like both TLK1 and TLK2.²⁶ CHD8 spectra were detected at similar levels between TLK2-WT and TLK2-D551G, which retains some activity, but were reduced with the kinase dead TLK2-S617L (figures 4C,D and 5). In contrast, CHD7 spectra were highest in cells expressing TLK2-D551G. We performed BioID-Westerns to validate these

Figure 6

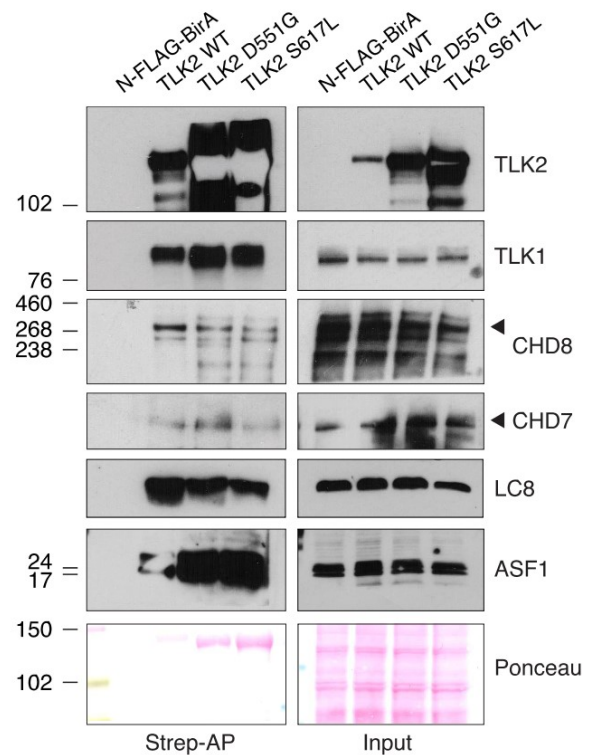


Figure 6 Validation of proximal interactions with CHD7 and CHD8. Western blot analyses of the indicated proteins from Strep-affinity purification (AP) lysates from AD-293 cells transfected with the indicated BioID construct and supplemented with biotin. Input levels are shown and ponceau stained blots provided as a loading control. Representative data from two biological replicates is shown.

proximal interactions and their relative differences. Expression of the control N-FLAG-BirA and biotin supplementation led to no detectable CHD7 or CHD8 detected in western blot analyses of Strep-AP protein lysates (figure 6). In contrast, both CHD7 and CHD8 were clearly validated with all TLK2 alleles, although CHD8 levels were lowest with S617L and CHD7 highest in TLK2-D551G, consistent with the MS data. As expected from the BioID-MS, TLK1 co-purified with all TLK2 alleles to a similar degree. It was also notable that the substrates, ASF1A and ASF1B, were highest with D551G and similar between TLK2-WT and TLK2-S617L, despite the much higher level of TLK2-S617L expression. These results indicate the missense mutations have differential effects on both proximal interactions and TLK-ASF1 interactions.

DISCUSSION

To our knowledge, at least 13 *TLK2* missense variants have been reported in MRD57 cases,^{7,9,11} with mutations clustering in the PKD. Previously described patients showed ID in different range of severity, ASD, language delay, motor delay, gastrointestinal issues and dysmorphic facies as prevalent features.^{7,8} In our cases, we confirmed a high incidence of ID (4/4), language delay (4/6) and dysmorphic facial features (6/6). On the contrary, compared with the available clinical literature, we observed a

under-representation of gastrointestinal problems (0/6) and ASD (1/6). We also observed additional features, including difficulties in reading and writing (3/6) or in memory and transcription (3/6) and skeletal anomalies of the hands (1/6) and the feet (1/6).

Functional characterisation has been reported only for four variants in the PKD, (p.(His493Arg), p.(His518Arg), p.(Asp629Asn), p.(Arg720Ala)) and has shown at least a 50% reduction in enzymatic activity compared with WT protein.¹⁰ Our data further expands the characterisation of MRD57 missense mutations and reinforces the prevailing hypothesis that the majority of these impair TLK2 kinase activity. Both TLK2-D551G and TLK2-S617L showed profoundly impaired kinase activity, as well as altered subcellular localisation, the significance of which remains unclear (figure 3, online supplemental figures S3 and S4). As also suggested by *in silico* tools (online supplemental table S5), TLK2-S617L caused a more severe impairment of protein activity and localisation compared with TLK2-D551G mutant. It is interesting to note that case carrying p.(Asp617Leu) was characterised by a mild-to-severe ID, with a IQ (verbal IQ 63, non-verbal IQ 74) that was lower than the one observed in case carrying p.(Asp551Gly) variant and comparable to the one observed in patients carrying p.(Glu475Ter) variant (online supplemental table S6). Based on the limited available clinical information, we could therefore suggest that the higher impairment of the protein activity mediated by p.(Ser617Leu) variant could be reflected on the clinical side by a more severe phenotype.

Both mutants overexpressed in AD-293 cells showed higher expression compared with WT. Accordingly, LCLs carrying p.(Asp551Gly) variant showed significantly higher TLK2 protein levels compared with control. Surprisingly, the higher protein expression was counterbalanced by drastically reduced mRNA levels, suggesting a potential negative feedback control, further causing reduced *TLK2* total mRNA levels.

Despite the severe effects on kinase activity caused by the heterozygous missense mutations identified in MRD57 patients to date, monoallelic *Tlk2* loss did not cause overt phenotypes in mice, but neurodevelopment and behaviour were not assessed in these animals.⁵ Given that TLK2 dimerises with both TLK1 and TLK2 and this is important for its activity, it is also likely that kinase impaired mutants exert some dominant negative effects that contribute to an overall phenotype that is more severe than haploinsufficiency.³¹ The recent identification of multiple MRD57 cases with *TLK2* haploinsufficiency suggests that an in-depth evaluation of neurodevelopment is needed in mice with reduced *Tlk2* levels to determine if they represent a model of MRD57. The placental issues observed in mice with homozygous deletion of *Tlk2* were not identified in *Tlk2* heterozygous mice, but human gestation is considerably longer, and more subtle placental issues could be present. Recent work showed that total TLK depletion leads to an innate immune secretory response in cancer cells and mice.^{2 6 32} Maternal immune activation has been implicated in ASD and associated with placental defects in mice, suggesting that impaired chromatin maintenance and epigenetic dysregulation could potentially underlie the pathological effects of TLK2 haploinsufficiency.^{2 33 34} This is consistent with the increased chromatin accessibility reported here in TLK2-D551G patient cells (figure 2B–E), as well as the strong enrichment of chromatin proteins in the TLK2 interactome in the SFARI and DECIPHER databases.

Many genes encoding proteins involved in chromatin remodelling are associated with neurodevelopmental disorders. TLK2, as well as the missense mutants we tested, showed proximal interactions with many of them, including CHD8 and CHD7,

that are mutated in ASD and CHARGE syndrome. In addition to these proteins, both TLK2 missense mutants showed altered interactions with additional proteins implicated in neurodevelopment. This included RAD50, a part of the MRE11-RAD50-NBS1 DNA repair complex that localises to replication forks and plays a key role in DNA-double-strand break repair.³⁵ *RAD50* mutations, present in the DECIPHER database, underlie Nijmegen breakage syndrome-like disorder (MIM# 613078). This condition is characterised by microcephaly, which is also commonly observed in many patients with *TLK2* variants. Furthermore, *RAD50* proximal interactions were reduced with both missense mutants, potentially suggesting reduced localisation to replication forks (figure 5).³⁶ Similarly, *YEATS2*, a chromatin reader component, is suggested as an ASD-associated gene by de novo genetic risk analysis and GWAS (SFARI database criteria 3.1, suggestive evidence),^{37 38} was linked to epilepsy and was enriched with TLK2-WT compared with either missense mutant.^{39–41} In contrast, *ZNF148* and *PAPOLG*, that are also associated with neurodevelopmental disorders, were strongly enriched with both missense mutants and detected at very low levels with TLK2-WT, while other SFARI genes, including *BRD4*, *JMJD1C*, *MSANTD2*, *CCNK* and *NACC1* were reduced specifically with the less active TLK2-S617L variant. In future work, it will be of interest to examine the potential functional relevance of these interactions to determine if their alterations underlie the altered chromatin state we observed in LCLs from case 1 or other phenotypes associated with TLK2 loss of function. This approach may detect new candidate genes involved in neurodevelopmental disorders or help us understand the involvement of this network of SFARI genes in isolated or syndromic ASD and ID.

The knowledge of altered protein interactomes is important to understand the molecular impact of disease mutations and could be helpful in identifying pharmacological treatments to mitigate more severe phenotypes, such as epileptic seizures. It is attractive to imagine the possibility of repurposing drugs able to modulate the functions of some genes to influence their impact on disease pathology.⁴²

In conclusion, we provided the clinical description of six new cases carrying likely pathogenic and pathogenic *TLK2* variants and we presented new insights into the impact of *TLK2* missense variants, observing impairment in kinase activity, localisation and interaction (online supplemental figure S4). Our work offers a deep characterisation of two missense variants localised in a key domain of the TLK2 protein, where most mutations related to MRD57 disorder occur, providing new insights into the potential role TLK2 in neurodevelopmental disorders.

Author affiliations

¹Department of Medical Sciences, University of Turin, Torino, Italy

²Institute of Human Genetics and Center for Molecular Medicine Cologne, University of Cologne, Cologne, Germany

³The Barcelona Institute of Science and Technology, Institute for Research in Biomedicine, Barcelona, Spain

⁴Department of Environment and Health, Istituto Superiore di Sanità, Roma, Italy

⁵Genetics and Rare Diseases Research Division, Ospedale Pediatrico Bambino Gesù IRCCS, Roma, Italy

⁶Department of Oncology and Molecular Medicine, Istituto Superiore di Sanità, Rome, Italy

⁷Medical Genetics Unity, Sant'Orsola-Malpighi University Hospital, Bologna, Italy

⁸Department of Pediatrics and Public Health and Pediatric Sciences, University of Turin, Torino, Italy

⁹Department of Molecular Medicine, University of Pavia, Pavia, Italy

¹⁰Department of Sciences for Health Promotion and Mother and Child Care "G. D'Alessandro", University of Palermo, Palermo, Italy

¹¹Department of Genetics, Reference center for Rare Diseases and Developmental Anomalies, Caen, France

- ¹²Seaver Autism Center for Research and Treatment, Icahn School of Medicine at Mount Sinai, New York City, New York, USA
- ¹³Department of Psychiatry, Icahn School of Medicine at Mount Sinai, New York City, New York, USA
- ¹⁴The Mindich Child Health and Development Institute, Icahn School of Medicine at Mount Sinai, New York City, New York, USA
- ¹⁵Friedman Brain Institute, Icahn School of Medicine at Mount Sinai, New York City, New York, USA
- ¹⁶Department of Medical and Surgical Sciences, University of Bologna, Bologna, Italy
- ¹⁷Department of Genetics and Genomic Sciences, Icahn School of Medicine at Mount Sinai, New York City, New York, USA
- ¹⁸Department of Neuroscience, Icahn School of Medicine at Mount Sinai, New York City, New York, USA
- ¹⁹Department of Oncology and Molecular Medicine, Istituto Superiore di Sanità, Roma, Italy
- ²⁰Radiation Oncology Branch, National Cancer Institute, Bethesda, Maryland, USA
- ²¹Unit of Medical Genetics, "Città della Salute e della Scienza" University Hospital, Torino, Italy

Twitter Lisa Pavinato @lisapavinato

Acknowledgements The authors would like to thank the patients and their families for their precious collaboration.

Contributors MV-P, MSC, MG, MV and GA-G performed activity, localisation and BioID-MS analysis. LP wrote and edited the manuscript, interpreted exome data, collected the cases and performed variant confirmation, mRNA and splicing analysis. CA and VP performed the SCGE assay. EG interpreted exome data. DC, VAMG, KR, CC and GBF followed patients and collected their clinical information. SDR and JB performed exome sequencing. AB, TP, PD, AC, FCR and MT processed and analysed the WES data. THS and AB designed and supervised the project, analyzed data and wrote the manuscript.

Funding This research received funding specifically appointed to Department of Medical Sciences from the Italian Ministry for Education, University and Research (Ministero dell'Istruzione, dell'Università e della Ricerca—MIUR) under the programme 'Dipartimenti di Eccellenza 2018–2022' Project code D15D18000410001. MV-P was funded by an FPI fellowship from the Ministry of Science, Innovation and Universities (MCIU) and MSC by a Masters fellowship from the BIST and support from the IRB Barcelona. THS was funded by the MCIU (PGC2018-095616-B-I00/GINDATA and FEDER). MT was funded by Fondazione Bambino Gesù (Vite Coraggiose). The whole exome sequencing was performed as part of the Autism Sequencing Consortium and was supported by the NIMH (MH111661). Thanks to the MSPCF of IRB Barcelona, a principal unit in Proteored, PRB3, supported by PT17/0019 of the PE I+D+i 2013-2016, funded by SCIII and ERDF. This study makes use of data generated by the DECIPHER community. A full list of centres that contributed to the generation of the data is available from: <http://decipher.sanger.ac.uk> and via email from: decipher@sanger.ac.uk. Funding for the project was provided by the Wellcome Trust.

Competing interests None declared.

Patient consent for publication Parental/Guardian consent obtained.

Ethics approval The study protocol was approved by the internal Ethics Committee, according to the Declaration of Helsinki and informed consent was obtained from participating families.

Provenance and peer review Not commissioned; externally peer reviewed.

Data availability statement Data are available in a public, open access repository or included in the article or uploaded as supplementary information.

Supplemental material This content has been supplied by the author(s). It has not been vetted by BMJ Publishing Group Limited (BMJ) and may not have been peer-reviewed. Any opinions or recommendations discussed are solely those of the author(s) and are not endorsed by BMJ. BMJ disclaims all liability and responsibility arising from any reliance placed on the content. Where the content includes any translated material, BMJ does not warrant the accuracy and reliability of the translations (including but not limited to local regulations, clinical guidelines, terminology, drug names and drug dosages), and is not responsible for any error and/or omissions arising from translation and adaptation or otherwise.

ORCID iDs

Lisa Pavinato <http://orcid.org/0000-0002-7630-8365>
 Marina Villamor-Payà <http://orcid.org/0000-0002-7288-4197>
 Alessandro Bruselles <http://orcid.org/0000-0002-1556-4998>
 Diana Carli <http://orcid.org/0000-0001-5690-6504>
 Elisa Giorgio <http://orcid.org/0000-0003-4076-4649>
 Francesca Clementina Radio <http://orcid.org/0000-0003-1993-8018>
 Kara Ranguin <http://orcid.org/0000-0002-9732-8090>
 Travis H Stracker <http://orcid.org/0000-0002-8650-2081>

Alfredo Brusco <http://orcid.org/0000-0002-8318-7231>

REFERENCES

- Lee S-B, Segura-Bayona S, Villamor-Payà M, Saredi G, Todd MAM, Attolini CS-O, Chang T-Y, Stracker TH, Groth A. Tausled-like kinases stabilize replication forks and show synthetic lethality with checkpoint and PARP inhibitors. *Sci Adv* 2018;4.
- Segura-Bayona S, Stracker TH. The Tausled-like kinases regulate genome and epigenome stability: implications in development and disease. *Cell Mol Life Sci* 2019;76:3827–41.
- Bruinsma W, van den Berg J, Aprelia M, Medema RH. Tausled-like kinase 2 regulates recovery from a DNA damage-induced G2 arrest. *EMBO Rep* 2016;17:659–70.
- Klimovskaia IM, Young C, Strømme CB, Menard P, Jasencakova Z, Mejlvang J, Ask K, Ploug M, Nielsen ML, Jensen ON, Groth A. Tausled-like kinases phosphorylate ASF1 to promote histone supply during DNA replication. *Nat Commun* 2014;5:3394.
- Segura-Bayona S, Nobel PA, González-Burón H, Youssef SA, Peña-Blanco A, Coyaud Étienne, López-Rovira T, Rein K, Palenzuela L, Colombelli J, Forrow S, Raught B, Groth A, de Bruin A, Stracker TH. Differential requirements for Tausled-like kinases 1 and 2 in mammalian development. *Cell Death Differ* 2017;24:1872–85.
- Segura-Bayona S, Villamor-Payà M, Attolini CS-O, Stracker TH. Tausled-like kinase activity is required for transcriptional silencing and suppression of innate immune signaling 2019.
- Reijnders MRF, Miller KA, Alvi M, Goos JAC, Lees MM, de Burca A, Henderson A, Kraus A, Mikat B, de Vries BBA, Isidor B, Kerr B, Marcelis C, Schluth-Bolard C, Deshpande C, Ruivenkamp CAL, Wiczorek D, Baralle D, Blair EM, Engels H, Lüdecke H-J, Eason J, Santen GWE, Clayton-Smith J, Chandler K, Tatton-Brown K, Payne K, Helbig K, Radtke K, Nugent KM, Cremer K, Strom TM, Bird LM, Sinnema M, Bitner-Glindzic M, van Dooren MF, Alders M, Koopmans M, Brick L, Kozenko M, Harline ML, Klaassens M, Steinraths M, Cooper NS, Edery P, Yap P, Terhal PA, van der Spek PJ, Lakeman P, Taylor RL, Littlejohn RO, Pfundt R, Mercimek-Andrews S, Stegmann APA, Kant SG, McLean S, Joss S, Swagemakers SMA, Douzou S, Wall SA, Küry S, Calpena E, Koelling N, McGowan SJ, Twigg SRF, Mathijssen IMJ, Nellaker C, Brunner HG, Wilkie AOM, Novo D, Deciphering Developmental Disorders Study. De novo and inherited loss-of-function variants in TLK2: clinical and genotype-phenotype evaluation of a distinct neurodevelopmental disorder. *Am J Hum Genet* 2018;102:1195–203.
- Töpf A, Oktay Y, Balaraçu S, Yilmaz E, Sonmezler E, Yis U, Laurie S, Thompson R, Roos A, MacArthur DG, Yaramis A, Gungör S, Lochmüller H, Hiz S, Horvath R. Severe neurodevelopmental disease caused by a homozygous TLK2 variant. *Eur J Hum Genet* 2019.
- Lielieveld SH, Reijnders MRF, Pfundt R, Yntema HG, Kamsteeg E-J, de Vries P, de Vries BBA, Willemsen MH, Kleefstra T, Löhner K, Vreburg M, Stevens SJ, van der Burg I, Bongers EMHF, Stegmann APA, Rump P, Rinne T, Nelen MR, Veltman JA, Vissers LELM, Brunner HG, Gillissen C. Meta-Analysis of 2,104 trios provides support for 10 new genes for intellectual disability. *Nat Neurosci* 2016;19:1194–6.
- Mortuza GB, Hermida D, Pedersen A-K, Segura-Bayona S, López-Méndez B, Redondo P, Rüter P, Pozdnyakova I, Garrote AM, Muñoz IG, Villamor-Payà M, Jauset C, Olsen JV, Stracker TH, Montoya G. Molecular basis of Tausled-Like kinase 2 activation. *Nat Commun* 2018;9:2535.
- Satterstrom FK, Kosmicki JA, Wang J, Breen MS, De Rubeis S, An J-Y, Peng M, Collins R, Grove J, Klei L, Stevens C, Reichert J, Mulhern MS, Artomov M, Gerges S, Sheppard B, Xu X, Bhaduri A, Norman U, Brand H, Schwartz G, Nguyen R, Guerrero EE, Dias C, Betancur C, Cook EH, Gallagher L, Gill M, Sutcliffe JS, Thurm A, Zwick ME, Borglum AD, State MW, Cicek AE, Talkowski ME, Cutler DJ, Devlin B, Sanders SJ, Roeder K, Daly MJ, Buxbaum JD, Aleksic B, Anney R, Barbosa M, Bishop S, Brusco A, Bybjerg-Grauholm J, Carracedo A, Chan MCY, Chiochetti AG, Chung BHY, Coo H, Cuccaro ML, Curró A, Dalla Bernardina B, Doan R, Domenici E, Dong S, Fallerini C, Fernández-Prieto M, Ferrero GB, Freitag CM, Fromer M, Gargus JJ, Geschwind D, Giorgio E, González-Peñas J, Guter S, Halpern D, Hansen-Kiss E, He X, Herman GE, Hertz-Picciotto I, Hougaard DM, Hultman CM, Ionita-Laza I, Jacob S, Jamison J, Jugessur A, Kaartinen M, Knudsen GP, Kolevzon A, Kushima I, Lee SL, Lehtimäki T, Lim ET, Lintas C, Lipkin WI, Lopergolo D, Lopes F, Ludena Y, Maciel P, Magnus P, Mahjani B, Maltman N, Manoach DS, Meiri G, Menashe I, Miller J, Minshew N, Montenegro EMS, Moreira D, Morrow EM, Mors O, Mortensen PB, Mosconi M, Muglia P, Neale BM, Nordentoft M, Ozaki N, Palotie A, Paralleda M, Passos-Bueno MR, Pericak-Vance M, Persico AM, Pessah I, Puura K, Reichenberg A, Renieri A, Riberi E, Robinson EB, Samocha KE, Sandin S, Santangelo SL, Schellenberg G, Scherer SW, Schlitt S, Schmidt R, Schmitt L, Silva IMW, Singh T, Siper PM, Smith M, Soares G, Stoltenberg C, Suren P, Susser E, Sweeney J, Szatmari P, Tang L, Tassone F, Teufel K, Trabetti E, Autism Sequencing Consortium, iPSYCH-Broad Consortium. Large-Scale exome sequencing study implicates both developmental and functional changes in the neurobiology of autism. *Cell* 2020;180:568–84. doi:10.1016/j.cell.2019.12.036
- Iossifov I, O'Roak BJ, Sanders SJ, Ronemus M, Krumm N, Levy D, Stessman HA, Witherspoon KT, Vives L, Patterson KE, Smith JD, Paepel B, Nickerson DA, Dea J, Dong S, Gonzalez LE, Mandell JD, Mane SM, Murtha MT, Sullivan CA, Walker MF, Waqar Z, Wei L, Willsey AJ, Yamrom B, Lee Y-ha, Grabowska E, Dalkic E, Wang Z, Marks S, Andrews P, Leotta A, Kendall J, Hakker I, Rosenbaum J, Ma B, Rodgers L, Troge J, Narzisi G, Yoon S, Schatz MC, Ye K, McCombie WR, Shendure J, Eichler EE, State MW,

- Wigler M. The contribution of de novo coding mutations to autism spectrum disorder. *Nature* 2014;515:216–21.
- 13 O’Roak BJ, Deriziotis P, Lee C, Vives L, Schwartz JJ, Girirajan S, Karakoc E, Mackenzie AP, Ng SB, Baker C, Rieder MJ, Nickerson DA, Bernier R, Fisher SE, Shendure J, Eichler EE. Exome sequencing in sporadic autism spectrum disorders identifies severe de novo mutations. *Nat Genet* 2011;43:585–9.
 - 14 De Rubeis S, He X, Goldberg AP, Poultney CS, Samocha K, Cicek AE, Kou Y, Liu L, Fromer M, Walker S, Singh T, Klei L, Kosmicki J, Shih-Chen F, Aleksic B, Biscaldi M, Bolton PF, Brownfeld JM, Cai J, Campbell NG, Carracedo A, Chahrour MH, Chiocchetti AG, Coon H, Crawford EL, Curran SR, Dawson G, Duketis E, Fernandez BA, Gallagher L, Geller E, Guter SJ, Hill RS, Ionita-Laza J, Jimenez Gonzalez P, Kilpinen H, Klauck SM, Kolevzon A, Lee I, Lei J, Lei J, Lehtimäki T, Lin C-F, Ma’ayan A, Marshall CR, McInnes AL, Neale B, Owen MJ, Ozaki N, Parellada M, Parr JR, Purcell S, Puura K, Rajagopalan D, Rehnström K, Reichenberg A, Sato A, Sachse M, Sanders SJ, Schafer C, Schulte-Rüther M, Skuse D, Stevens C, Szatmari P, Tammimies K, Valladares O, Voran A, Li-San W, Weiss LA, Willsey AJ, Yu TW, Yuen RKC, Cook EH, Freitag CM, Gill M, Hultman CM, Lehner T, Palotie A, Schellenberg GD, Sklar P, State MW, Sutcliffe JS, Walsh CA, Scherer SW, Zwick ME, Baretz JC, Cutler DJ, Roeder K, Devlin B, Daly MJ, Buxbaum JD, DDD Study, Homozygosity Mapping Collaborative for Autism, UK10K Consortium. Synaptic, transcriptional and chromatin genes disrupted in autism. *Nature* 2014;515:209–15. doi:10.1038/nature13772
 - 15 Kopanos C, Tsiolkas V, Kouris A, Chapple CE, Albarca Aguilera M, Meyer R, Massouras A. VarSome: the human genomic variant search engine. *Bioinformatics* 2019;35:1978–80.
 - 16 Desmet F-O, Hamroun D, Lalande M, Collod-Béroud G, Claustres M, Béroud C. Human splicing finder: an online bioinformatics tool to predict splicing signals. *Nucleic Acids Res* 2009;37:e67.
 - 17 Flex E, Martinelli S, Van Dijk A, Cioffi A, Cecchetti S, Coluzzi E, Pannone L, Andreoli C, Radio FC, Pizzi S, Carpentieri G, Bruselles A, Catanzaro G, Pedace L, Miele E, Carcarino E, Ge X, Chijiwa C, Lewis MES, Meuwissen M, Kenis S, Van der Aa N, Larson A, Brown K, Wasserstein MP, Skotko BG, Begtrup A, Person R, Karayiorgou M, Roos JL, Van Gassen KL, Koopmans M, Bijlsma EK, Santen GWE, Barge-Schaapveld DQCM, Ruivenkamp CAL, Hoffer MJV, Lalani SR, Streff H, Craigen WJ, Graham BH, van den Elzen APM, Kamphuis DJ, Ünnap K, Reinson K, Pajusalu S, Wojcik MH, Viberti C, Di Gaetano C, Bertini E, Petrucci S, De Luca A, Rota R, Ferretti E, Matullo G, Dallapiccola B, Sgura A, Walkiewicz M, Kooy RF, Tartaglia M. Aberrant function of the C-terminal tail of HIST1H1E accelerates cellular senescence and causes premature aging. *Am J Hum Genet* 2019;105:493–508.
 - 18 Silva J, Aivio S, Knobel PA, Bailey LJ, Casali A, Vinaixa M, Garcia-Cao I, Coyaud Étienne, Jourdain AA, Pérez-Ferreros P, Rojas AM, Antolin-Fontes A, Samino-Gené S, Raught B, González-Reyes A, Ribas de Pouplana L, Doherty AJ, Yanes O, Stracker TH. EXD2 governs germ stem cell homeostasis and lifespan by promoting mitochondrial integrity and translation. *Nat Cell Biol* 2018;20:162–74.
 - 19 Firth HV, Richards SM, Bevan AP, Clayton S, Corvas M, Rajan D, Van Vooren S, Moreau Y, Pettett RM, Carter NP. Decipher: database of chromosomal imbalance and phenotype in humans using Ensembl resources. *Am J Hum Genet* 2009;84:524–33.
 - 20 Havrilla JM, Pedersen BS, Lyster RM, Quinlan AR. A map of constrained coding regions in the human genome. *Nat Genet* 2019;51:88–95. doi:10.1038/s41588-018-0294-6
 - 21 Manning KS, Cooper TA. The roles of RNA processing in translating genotype to phenotype. *Nat Rev Mol Cell Biol* 2017;18:102–14.
 - 22 Siwaszek A, Ukleja M, Dziembowski A. Proteins involved in the degradation of cytoplasmic mRNA in the major eukaryotic model systems. *RNA Biol* 2014;11:1122–36.
 - 23 Treiber DK, Shah NP. Ins and outs of kinase DFG motifs. *Chem Biol* 2013;20:745–6.
 - 24 Vijayan RSK, He P, Modi V, Duong-Ly KC, Ma H, Peterson JR, Dunbrack RL, Levy RM. Conformational analysis of the DFG-out kinase motif and biochemical profiling of structurally validated type II inhibitors. *J Med Chem* 2015;58:466–79.
 - 25 Roux KJ, Kim DI, Burke B, May DG. BioID: a screen for protein-protein interactions. *Curr Protoc Protein Sci* 2018;91:19.23.1–19.23.15.
 - 26 Wessel SR, Mohni KN, Luzwick JW, Dugrawala H, Cortez D. Functional analysis of the replication fork proteome identifies BET proteins as PCNA regulators. *Cell Rep* 2019;28:3497–509.
 - 27 Lalani SR, Safiullah AM, Fernbach SD, Harutyunyan KG, Thaller C, Peterson LE, McPherson JD, Gibbs RA, White LD, Hefner M, Davenport SLH, Graham JM, Bacino CA, Glass NL, Towbin JA, Craigen WJ, Neish SR, Lin AE, Belmont JW. Spectrum of CHD7 mutations in 110 individuals with CHARGE syndrome and genotype-phenotype correlation. *Am J Hum Genet* 2006;78:303–14.
 - 28 Bernier R, Golzio C, Xiong B, Stessman HA, Coe BP, Penn O, Witherspoon K, Gerdtz J, Baker C, Vulto-van Silfhout AT, Schuurs-Hoeijmakers JH, Fichera M, Bosco P, Buono S, Alberti A, Failla P, Peeters H, Steyaert J, Vissers LELM, Francescato L, Mefford HC, Rosenfeld JA, Bakken T, O’Roak BJ, Pawlus M, Moon R, Shendure J, Amaral DG, Lein E, Rankin J, Romano C, de Vries BBA, Katsanis N, Eichler EE. Disruptive CHD8 mutations define a subtype of autism early in development. *Cell* 2014;158:263–76.
 - 29 Manning BJ, Yusufzai T. The ATP-dependent chromatin remodeling enzymes CHD6, CHD7, and CHD8 exhibit distinct nucleosome binding and remodeling activities. *J Biol Chem* 2017;292:11927–36.
 - 30 Murawska M, Brehm A. CHD chromatin remodelers and the transcription cycle. *Transcription* 2011;2:244–53.
 - 31 Sunavala-Dossabhoy G, Li Y, Williams B, De Benedetti A. A dominant negative mutant of TLK1 causes chromosome missegregation and aneuploidy in normal breast epithelial cells. *BMC Cell Biol* 2003;4:16.
 - 32 Liu H, Dowdle JA, Khurshid S, Sullivan NJ, Bertos N, Rambani K, Mair M, Daniel P, Wheeler E, Tang X, Toth K, Lause M, Harrigan ME, Eiring K, Sullivan C, Sullivan MJ, Chang SW, Srivastava S, Conway JS, Kladney R, McElroy J, Bae S, Lu Y, Tofigh A, Saleh SMI, Fernandez SA, Parvin JD, Coppola V, Macrae ER, Majumder S, Shapiro CL, Yee LD, Ramaswamy B, Hallett M, Ostrowski MC, Park M, Chamberlin HM, Leone G. Discovery of stromal regulatory networks that suppress Ras-Sensitized epithelial cell proliferation. *Dev Cell* 2017;41:392–407.
 - 33 Lombardo MV, Moon HM, Su J, Palmer TD, Courchesne E, Pramparo T. Maternal immune activation dysregulation of the fetal brain transcriptome and relevance to the pathophysiology of autism spectrum disorder. *Mol Psychiatry* 2018;23:1001–13.
 - 34 Carpentier PA, Dingman AL, Palmer TD. Placental TNF- α signaling in illness-induced complications of pregnancy. *Am J Pathol* 2011;178:2802–10.
 - 35 Taylor AM. Chromosome instability syndromes. *Best Pract Res Clin Haematol* 2001;14:631–44.
 - 36 Waltes R, Kalb R, Gatei M, Kijas AW, Stumm M, Soback A, Wieland B, Varon R, Lerehthal Y, Lavin MF, Schindler D, Dörk T. Human Rad50 deficiency in a Nijmegen breakage syndrome-like disorder. *Am J Hum Genet* 2009;84:605–16.
 - 37 Ruzzo EK, Pérez-Cano L, Jung J-Y, Wang L-K, Kashef-Haghighi D, Hartl C, Singh C, Xu J, Hoekstra JN, Leventhal O, Leppä VM, Gandal MJ, Paskov K, Stockham N, Polioudakis D, Lowe JK, Prober DA, Geschwind DH, Wall DP. Inherited and de novo genetic risk for autism impacts shared networks. *Cell* 2019;178:850–66.
 - 38 Anney R, Klei L, Pinto D, Almeida J, Bacchelli E, Baird G, Bolshakova N, Bölte S, Bolton PF, Bourgeron T, Brennan S, Brian J, Casey J, Conroy J, Correia C, Corsello C, Crawford EL, de Jonge M, Delorme R, Duketis E, Duque F, Estes A, Farrar P, Fernandez BA, Folstein SE, Fombonne E, Gilbert J, Gillberg C, Glessner JT, Green A, Green J, Guter SJ, Heron EA, Holt R, Howe JL, Hughes G, Hus V, Iglizoi R, Jacob S, Kenny GP, Kim C, Kolevzon A, Kustanovich V, Lajonchere CM, Lamb JA, Law-Smith M, Leboyer M, Le Couteur A, Leventhal BL, Liu X-Q, Lombard F, Lord C, Lotsepeich L, Lund SC, Magalhaes TR, Mantoulan C, McDougle CJ, Melhem NM, Merikangas A, Minschew NJ, Mirza GK, Munson J, Noakes J, Nygren G, Papanikolaou K, Pagnamenta AT, Parrini B, Paton T, Pickles A, Posey DJ, Poustka F, Ragoussis J, Regan R, Roberts W, Roeder K, Roge B, Rutter ML, Schliitt S, Shah N, Sheffield VC, Soorya L, Sousa I, Stoppioni V, Sykes N, Tancredi R, Thompson AP, Thomson S, Tryfon A, Tsiantis J, Van Engeland H, Vincent JB, Volkmar F, Vorstman JAS, Wallace S, Wing K, Wittmeyer K, Wood S, Zurawiecki D, Zwaigenbaum L, Bailey AJ, Battaglia A, Cantor RM, Coon H, Cuccaro ML, Dawson G, Ennis S, Freitag CM, Geschwind DH, Haines JL, Klauck SM, McMahon WM, Maestrini E, Miller J, Monaco AP, Nelson SF, Nurnberger JL, Oliveira G, Parr JR, Pericak-Vance MA, Piven J, Schellenberg GD, Scherer SW, Vicente AM, Wassink TH, Wijsman EM, Betancur C, Buxbaum JD, Cook EH, Gallagher L, Gill M, Hallmayer J, Paterson AD, Sutcliffe JS, Szatmari P, Vieland VJ, Hakonarson H, Devlin B. Individual common variants exert weak effects on the risk for autism spectrum disorders. *Hum Mol Genet* 2012;21:4781–92.
 - 39 Mi W, Guan H, Liu J, Zhao D, Xi Y, Jiang S, Andrews FH, Wang X, Gagea M, Wen H, Tora L, Dent SYR, Kutateladze TG, Li W, Li H, Shi X. YEATS2 links histone acetylation to tumorigenesis of non-small cell lung cancer. *Nat Commun* 2017;8:1088.
 - 40 Zhao D, Guan H, Zhao S, Mi W, Wen H, Li Y, Zhao Y, Allis CD, Shi X, Li H. YEATS2 is a selective histone crotonylation reader. *Cell Res* 2016;26:629–32. doi:10.1038/cr.2016.49
 - 41 Yeetong P, Pongpanich M, Srichomthong C, Assawapitaksakul A, Shotelersuk V, Tantirukdham N, Chunharas C, Suphapeetiporn K, Shotelersuk V. TTCCA repeat insertions in an intron of YEATS2 in benign adult familial myoclonic epilepsy type 4. *Brain Published Online First* 2019.
 - 42 Tranfaglia MR, Thibodeaux C, Mason DJ, Brown D, Roberts I, Smith R, Williams T, Cogram P. Repurposing available drugs for neurodevelopmental disorders: the fragile X experience. *Neuropharmacology* 2019;147:74–86.
 - 43 Szklarczyk D, Gable AL, Lyon D, Junge A, Wyder S, Huerta-Cepas J, Simonovic M, Doncheva NT, Morris JH, Bork P, Jensen LJ, Mering CV, von Mering C. STRING v11: protein-protein association networks with increased coverage, supporting functional discovery in genome-wide experimental datasets. *Nucleic Acids Res* 2019;47:D607–13.
 - 44 Oughtred R, Stark C, Breitkreutz B-J, Rust J, Boucher L, Chang C, Kolas N, O’Donnell L, Leung G, McAdam R, Zhang F, Dolma S, Willems A, Coulombe-Huntington J, Chatri-Aryamontri A, Dolinski K, Tyers M. The BioGRID interaction database: 2019 update. *Nucleic Acids Res* 2019;47:D529–41.
 - 45 Knight JDR, Choi H, Gupta GD, Pelletier L, Raught B, Nesvizhskii AI, Gingras A-C. ProHits-viz: a suite of web tools for visualizing interaction proteomics data. *Nat Methods* 2017;14:645–6.